Ship observations of stratocumulus clouds and drizzle in VOCALS

Simon de Szoeke[1], Sandra Yuter[2], Chris Fairall[3], Paquita Zuidema[4], Christina Aldereguia[2]

[1]Oregon State University; [2]North Carolina State University; [3]NOAA ESRL Physical Sciences Division, Boulder; [4]University of Miami

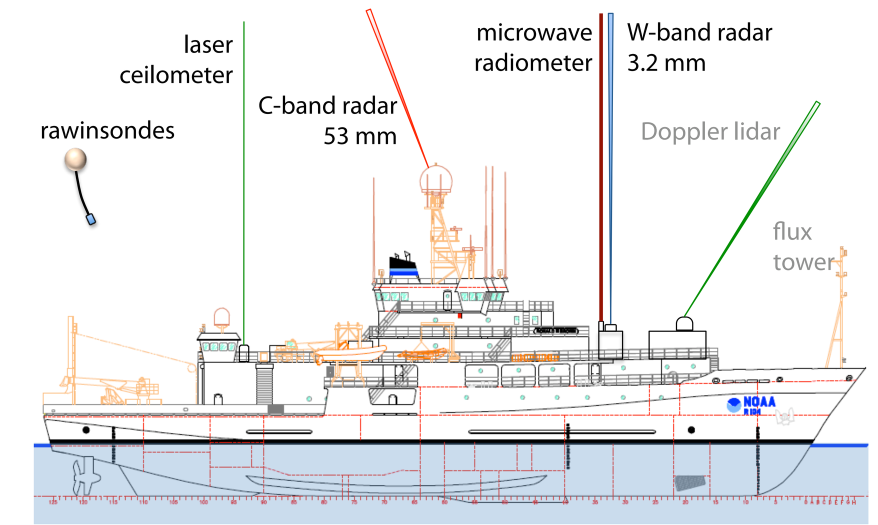

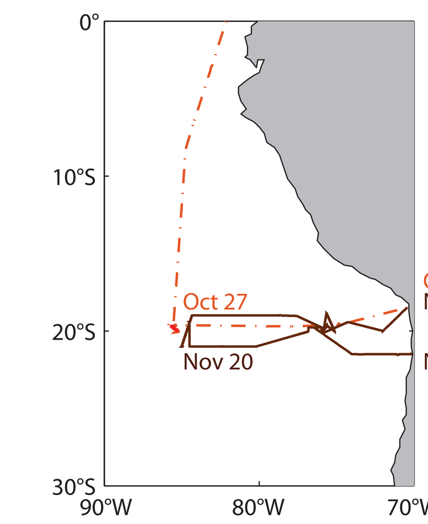

A13J-0428
AGU Fall 2009

1. Summary

Extensive stratocumulus clouds cover the southeastern tropical Pacific Ocean, cooling the ocean surface by shading it from the sun. Although this cloud deck is important to the climate, it is poorly simulated by climate models, in part because it is poorly understood. Drizzling cloud cells too small to be resolved by regional and global models contribute to the dynamics and microphysics of the cloud deck.

This poster presents shipboard observations of the stratocumulus clouds and drizzle in the southeastern tropical Pacific from the VOCALS Regional Experiment (REx). Different cloud remote sensing instruments have different sensitivities to liquid water. An optical laser ceilometer estimated cloud fraction at 0.94. The less sensitive W-band cloud radar can detect 86% of the clouds the ceilometer detects.

High liquid water path, indicative of thick drizzling clouds, is found in scenes of broken and unbroken clouds. Drizzle is neither necessary nor sufficient for pockets of open-cell clouds (POCs): both drizzling and non-drizzling clouds are observed in open- and closed-cell scenes (Fig. 1). "Boundary cells" were rarely observed in 828 hours of marine stratocumulus cloud observations. Drizzle was detected within 60 km of the ship for 466 hours.

Soundings often show curious layers of temperature stratification overlying the inversion, while humidity retains its sharp gradient at cloud top. These layers above the inversion have consistent potential temperature stratification of about 34 K km^{-1}. We hypothesize that the 34 K km^{-1} layer is a transient temperature perturbation triggered by strong updrafts that overshoot the inversion, roughly analogous to deep convection penetrating the tropopause.

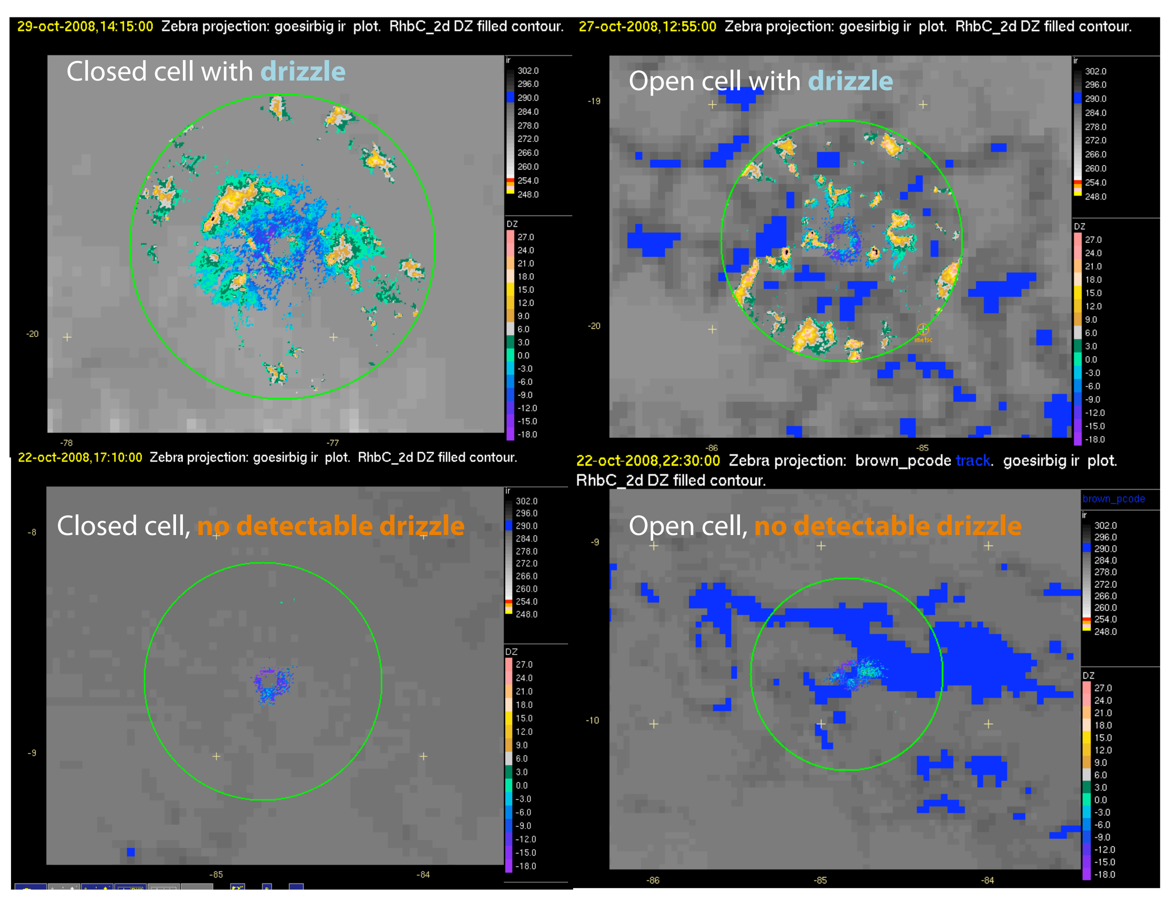

Figure 1. Four cases of C-band radar reflectivity (color shades) superimposed on infrared satellite images (grayscale). Significant drizzle is found in both closed- and open-cell mesoscale clouds (top images), and closed- and open-cells were also observed without detectable drizzle (bottom).

2. VOCALS REx ship measurements

The NOAA ship *Ronald H. Brown* made two research cruises to the southeastern tropical Pacific for VOCALS REx in October-November 2008. Investigators measured surface meteorology and air-sea fluxes. Observations from rawinsondes, radar, lidar, and passive radiometers provide statistics about the thermodynamics of the atmosphere and the distribution of clouds and rain in the marine stratocumulus deck (Table 1).

Table 1. Key measurements and sampling strategy of each instrument.

Instrument	measurement	sampling frequency	spatial range
rawinsondes	atm. pressure, temperature, humidity, and wind	4 hour	20 km profile
microwave radiometer	column water vapor and liquid	20 seconds	column integral
Doppler C-band radar	precipitation, mesoscale organization	10 minutes	60 km radius volume scan
Doppler W-band radar	clouds, precipitation, vertical velocity	10 minutes	12 km profile
ceilometer	cloud base height, cloud fraction	20 seconds	8 km
Doppler Lidar (HRDL)	wind, turbulence, and aerosol backscatter intensity	20 minutes	6 km radius volume & subcloud profile
solar and IR radiometers	surface downwelling radiative fluxes	10 minutes	in situ
surface turbulent fluxes	surface sensible heat flux, evaporation, wind stress vector	10 minutes	in situ

3. Cloud and drizzle

Mean cloud fraction for VOCALS REx leg 2 is 0.94 (Fig. 3). The ceilometer is more sensitive to clouds than the W-band radar. Cloud detection matches the radar for higher ceilometer backscatter thresholds but the thinnest 14% of clouds in VOCALS leg 2 are below W-band radar sensitivity. Liquid water path (LWP) is even less sensitive to thin clouds, and measures cloud and drizzle intensity.

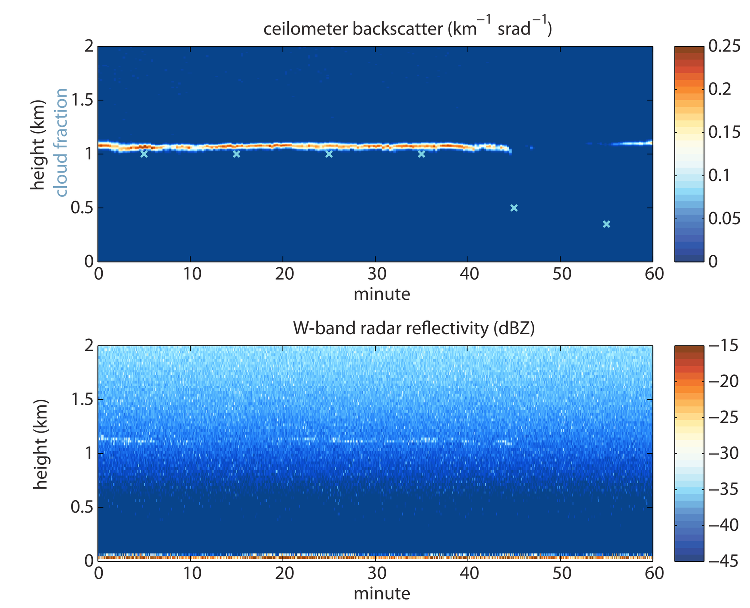

Figure 2. Ceilometer backscatter and W-band radar reflectivity for 2008 November 14, 20-21:00 UTC (15-16 local). Radar barely detects the very thin clouds in this case.

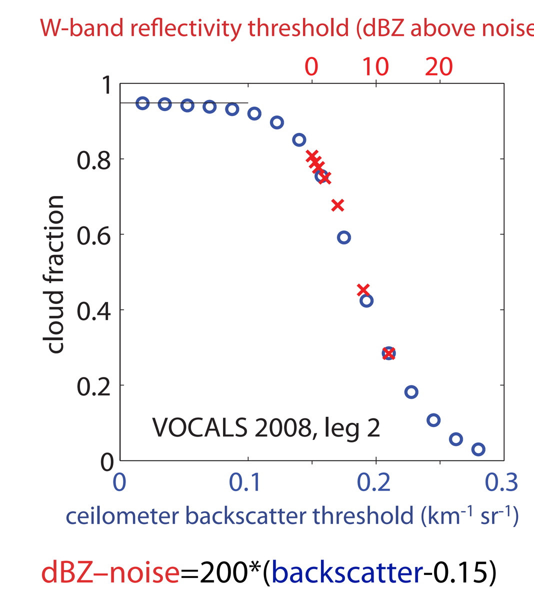

Figure 3. Cloud detection curves show the sensitivity of W-band radar (red xs) relative to the ceilometer (blue os). Black line is the automatic ceilometer cloud fraction.

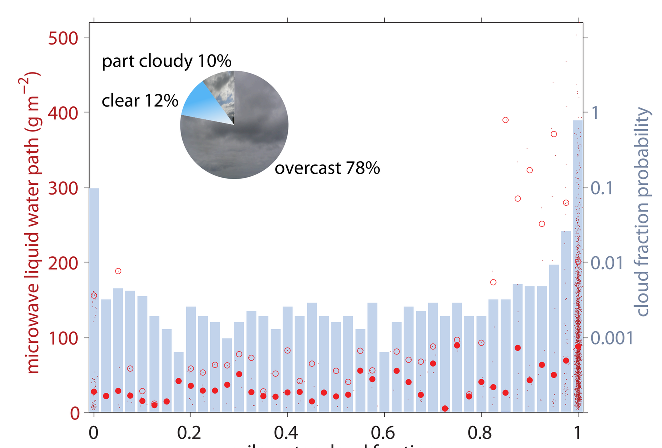

Figure 4. Probability of 10-minute cloud fraction in 0.025 cloud-fraction bins (bars). Liquid water path median (filled) and 90th percentile (open) binned by cloud fraction.

Cloud fraction depends on the area and time period over which it is computed. 10-minute ceilometer cloud fraction is bimodal (right logarithmic axis of Fig. 4). During Leg 2, 78% of the time the sky directly over the ship was overcast (cloud fraction=1) and 12% of the time was clear (cloud fraction=0). Averages of over 10 hours are needed to obtain significant frequencies of cloud fraction between 0 and 1. High LWP is found more commonly in overcast conditions but substantial LWP can also occur near clear areas (red dots, Fig. 4).

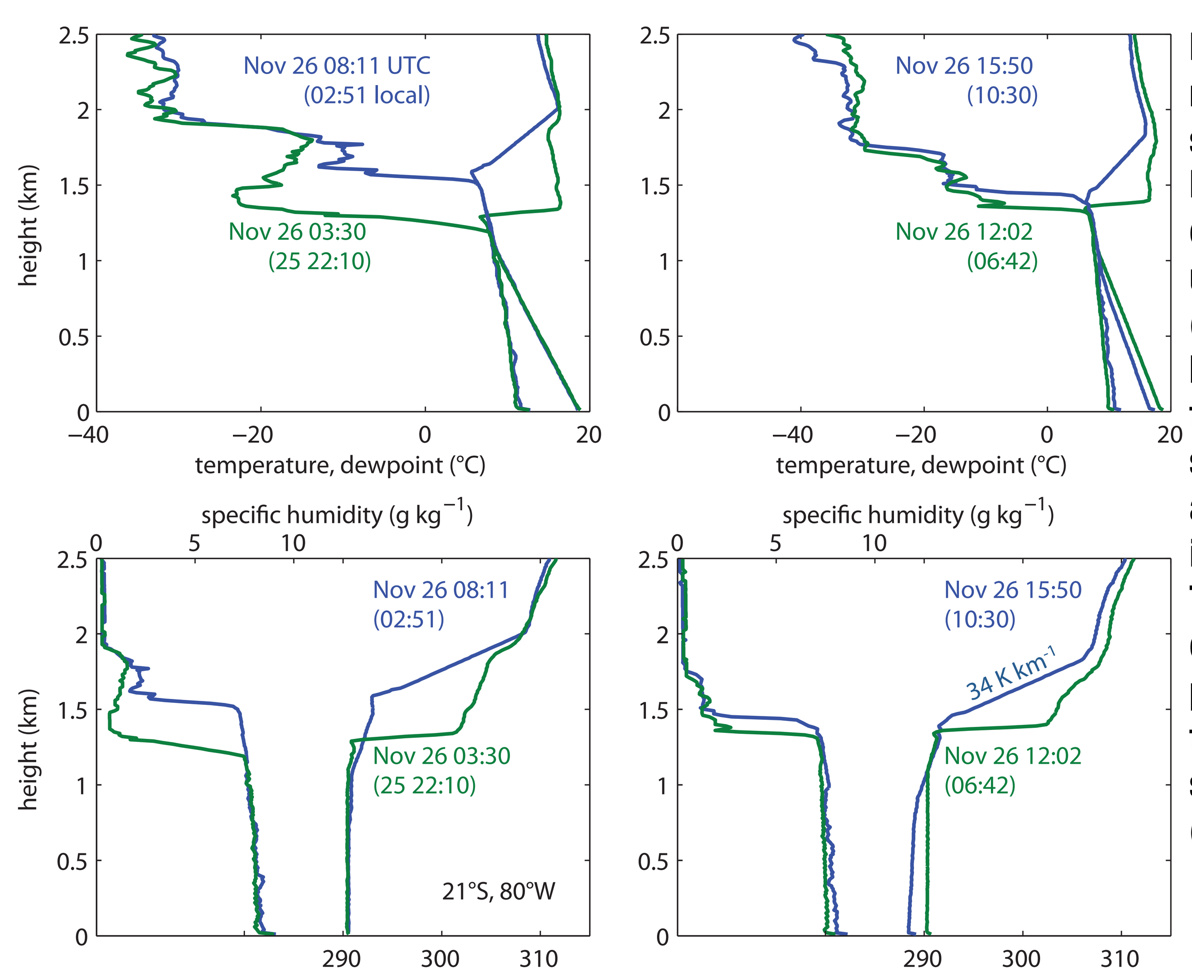

Figure 5. Four rawinsonde soundings from November 26 demonstrate usual conditions (green) followed by transient temperature stratification above the inversion (blue). Temperature and dew point (top 2 panels); potential temperature and specific humidity (bottom).

4. Inversions and interaction above the boundary layer

Figure 5 shows a series of four soundings, two with ordinary inversions (green), and two with transient (<4 hour) temperature stratification above the inversion (blue). Temperature and dew point show the saturated cloud and cloud top (upper panels). Potential temperature is a linear mixture between above-cloud-top and free-troposphere air in *34 K km^{-1} layers* above the inversion (lower Fig. 5). Specific humidity is indistinguishable from ordinary soundings in 34 K km^{-1} layers.

Temperature stratification from cloud top to the top of the stably stratified temperature layer is bimodal for VOCALS soundings (Figs. 6 & 7), with shallow strongly stable inversions distinguished from 34 K km^{-1} layers. Green lines for ordinary inversions with stability >65 °C km^{-1} are found at 1.0-1.4 km. 34 K km^{-1} layers can be higher and vary in thickness.

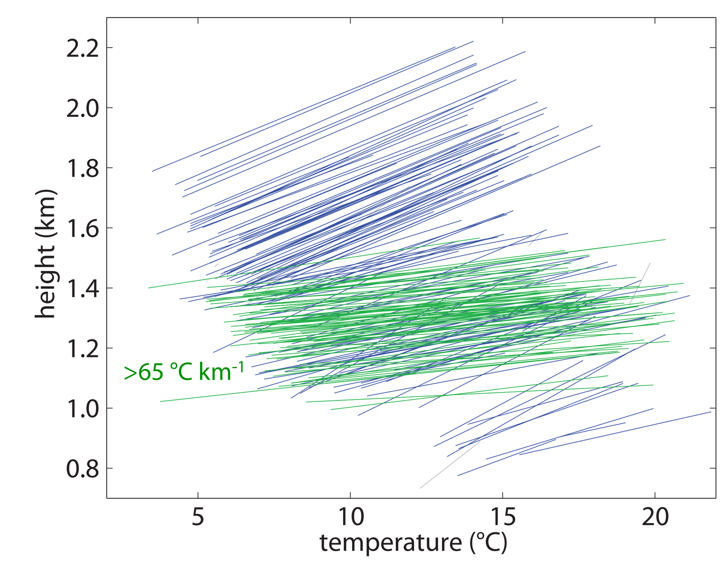

Figure 6. Composite overlay of temperature and height differences across inversions and 34 K km^{-1} layers.

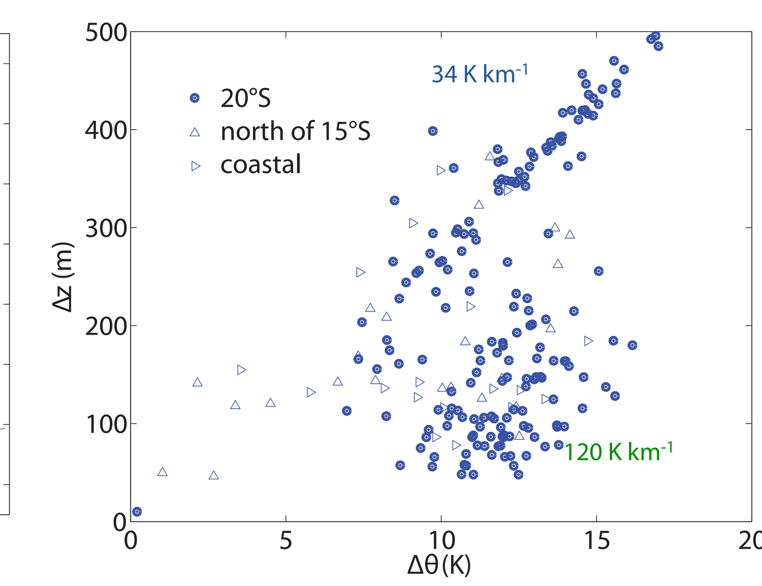

Figure 7. Potential temperature stability differentiates 34 K km^{-1} layers from inversions. Soundings outside the 75-85°W, 20°S region are plotted with triangles.

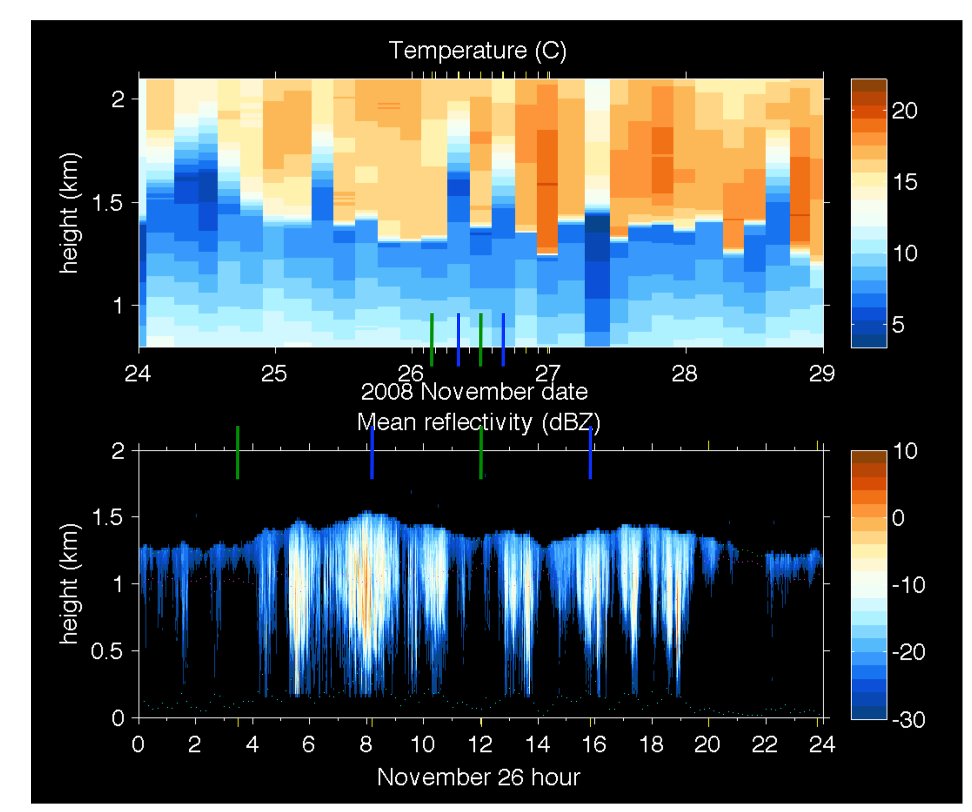

Figure 8. (Upper) 5-day time series of rawinsonde temperature soundings, color shaded. (Lower) Shaded reflectivity from the W-band cloud radar from November 26 UTC. Blue and green bars indicate the times of soundings in Fig. 5.

Five days of soundings from an active drizzle period reveal several 34 K km^{-1} layers (Fig. 8 upper). W-band radar reflectivity shows higher cloud top and stronger drizzle at times when 34 K km^{-1} layers above the inversion were observed. W-band cloud tops (Fig. 8 lower) are below the 34 K km^{-1} layer.

One hypothesis is that occasional strong updrafts associated with stronger drizzle overshoot the inversion (e.g. Fig. 9). The overshooting parcel cools adiabatically. Temperature perturbations mix with the environment by turbulence and spread horizontally by gravity waves. These transient perturbations dissipate within a few hours.

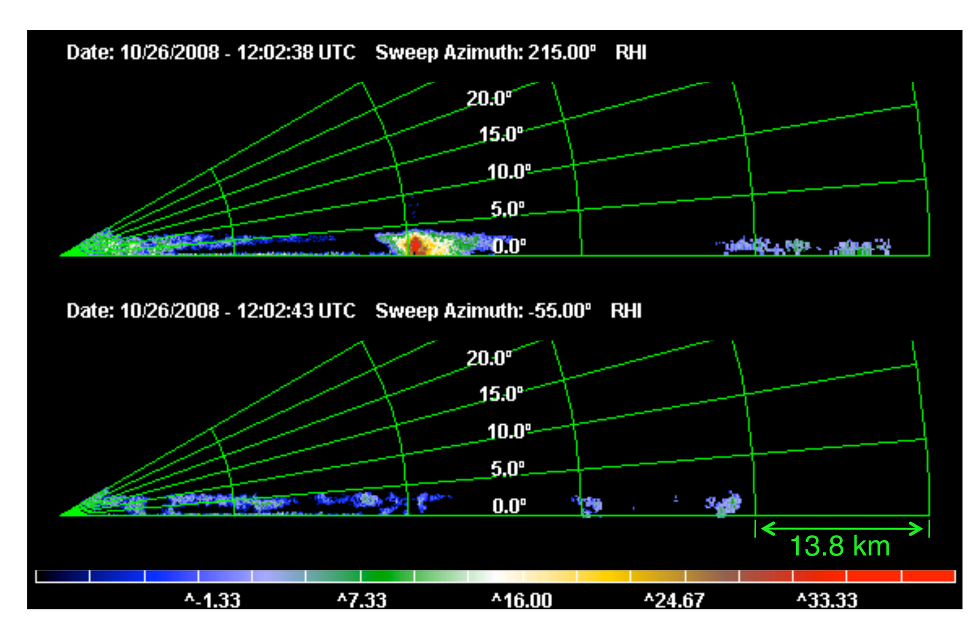

Figure 9. Two range-height indicator (RHI) scans from the NOAA C-band radar from *October* 26 12 UTC. Unusually strong convection 30 km from the ship in the top scan overshoots the mean cloud top height.